Cell, Vol. 81, 41–51, April 7, 1995, Copyright © 1995 by Cell Press

Hemostatic, Inflammatory, and Fibroblast Responses Are Blunted in Mice Lacking Gelsolin

Walter Witke,* Arlene H. Sharpe,† John H. Hartwig,* Toshifumi Azuma,* Thomas P. Stossel,* and David J. Kwiatkowski*
*Division of Experimental Medicine
Division of Hematology–Oncology
Department of Medicine
†Department of Pathology
Brigham and Women's Hospital
Harvard Medical School
Boston, Massachusetts 02115

Summary

Gelsolin, an 82 kDa actin-binding protein, has potent actin filament-severing activity in vitro. To investigate the in vivo function of gelsolin, transgenic gelsolin-null (*Gsn*$^-$) mice were generated and found to have normal embryonic development and longevity. However, platelet shape changes are decreased in *Gsn*$^-$ mice, causing prolonged bleeding times. Neutrophil migration in vivo into peritoneal exudates and in vitro is delayed. *Gsn*$^-$ dermal fibroblasts have excessive actin stress fibers and migrate more slowly than wild-type fibroblasts, but have increased contractility in vitro. These observations establish the requirement of gelsolin for rapid motile responses in cell types involved in stress responses such as hemostasis, inflammation, and wound healing. Neither gelsolin nor other proteins with similar actin filament-severing activity are expressed in early embryonic cells, indicating that this mechanism of actin filament dynamics is not essential for motility during early embryogenesis.

Introduction

Remodeling of the actin cytoskeleton is intrinsic to several cellular responses, including shape changes, chemotaxis, and secretion (Lee et al., 1993; Stossel, 1993; Condeelis, 1994). Numerous proteins control the assembly of cytoplasmic actin and the organization of actin filaments into a three-dimensional network (Hartwig and Kwiatkowski, 1991). One structurally related class of these proteins regulates actin filament length by severing preexisting filaments, capping the fast-growing filament end, or both (Weeds and Maciver, 1993) and is regulated by Ca^{2+} and phosphoinositides (PPIs). The family of actin filament–severing proteins includes gelsolin (Yin and Stossel, 1979), widely expressed in mammalian tissues (Kwiatkowski et al., 1988a; Kwiatkowski et al., 1988b); adseverin (also called scinderin), found primarily in adrenal glands (Maekawa et al., 1989); villin (Bretscher and Weber, 1980), a component of brush border microvilli; and possibly the recently described flightless I protein (Campbell et al., 1993), which has full-length homology to gelsolin, but has not yet been functionally characterized. F-actin-severing proteins with structural relationships to gelsolin have also been found in unicellular species, such as Dictyostelium discoideum (severin) (Yamamoto et al., 1982) and Physarum polycephalum (fragmin) (Hasegawa et al., 1980). By rupturing the noncovalent bonds among actin subunits in a filament, activation of a severing protein rapidly solates actin filament networks. After severing, gelsolin family members remain firmly attached to (or cap) the fast-exchanging (barbed) ends of the broken filament, thereby preventing annealing of ruptured filaments or growth by addition of actin monomers. Gelsolin can also nucleate actin polymerization from actin monomers in the presence of micromolar calcium ions or at pH 6.5 (Yin et al., 1981; Lamb et al., 1993). Gelsolin-capped actin filaments, whether generated through severing reactions or nucleation, are substrates for uncapping by interactions with PPI, leading to rapid actin assembly. Gelsolin has, therefore, a major potential role in modulating the viscosity of the cytoplasm during cell movement.

Circumstantial evidence supports the idea that gelsolin has an important role in cell motility. Gelsolin is particularly abundant in the cytoplasm of cells that locomote or change shape rapidly, such as blood platelets (Hartwig, 1992), neutrophils (Howard et al., 1990), and pulmonary macrophages (Yin and Stossel, 1979). Gelsolin expression is up-regulated when nonmotile cells differentiate and become more motile (Kwiatkowski, 1988; Diffenbach et al., 1989). Overexpression of gelsolin in NIH 3T3 fibroblasts leads to a dose-dependent increase in translocational motility as assessed by tissue culture wound closure and filter transmigration assays (Cunningham et al., 1991). Gelsolin–actin complexes form transiently during platelet (Kurth and Bryan, 1984; Lind et al., 1987), neutrophil (Howard et al., 1990), and macrophage activation (Chaponnier et al., 1987), accompanied by shuttling of gelsolin within the cell between membrane-bound and cytoplasmic locations (Hartwig, 1992). The presence and abundance of gelsolin (or a closely related homolog) in oocytes of Xenopus laevis has also suggested a role for gelsolin in early embryogenesis in vertebrates (Ankenbauer et al., 1988). However, the apparent normal motility of Dictyostelium mutants that lack the severing protein severin (André et al., 1989) has also suggested that in amoeba, individual actin filament–severing proteins may not be absolutely required for motility.

To determine the critical functions of gelsolin in a vertebrate organism in the presence of the numerous other proteins that also regulate actin assembly, we have generated gelsolin-null (*Gsn*$^-$) mice. We demonstrate physiological dysfunction during hemostasis, inflammation, and possibly tissue remodeling in animals lacking gelsolin. On the other hand, gelsolin is not necessary for oocyte development, sperm function, or embryogenesis. In wild-type mice, neither gelsolin nor other proteins with actin filament–severing activity are expressed early in embryonic development, suggesting that actin filament–capping proteins compensate at this developmental stage and that the mechanism of changes in the actin cytoskeleton is different in early embryonic cells.

A

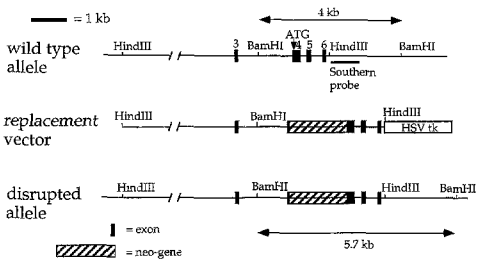

B

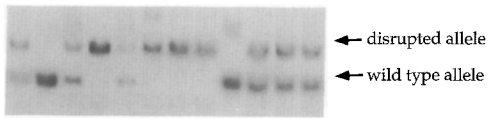

C

Cross	wild type	heteroz. (+/-)	homoz. (-/-)
(+/-) x (+/-)	19 (18%)	58 (56%)	26 (25%)
(-/-) x (-/-)			32 (litter size ~8)

Figure 1. Targeted Disruption of the *Gsn* Gene, Confirmation by Southern Blot Analysis, and Breeding Results

(A) The wild-type murine *Gsn* gene is shown on the first line, including exons 3–6, the initiator methionine of cytoplasmic gelsolin, and the probe used in Southern blot analysis. The second line shows the replacement vector constructed from a murine genomic *Gsn* clone, with insertion of the *neo*^{r} gene at a BglII site in exon 3, and attachment of the HSV–TK on the 3′ side. The third line shows the expected configuration of the *Gsn* gene following homologous recombination.

(B) Southern blot analysis of mouse tail DNA, following digestion with BamHI. Multiple progeny from a (+/−) × (+/−) breeding are analyzed.

(C) Breeding results of *Gsn*$^-$ heterozygotes and homozygotes.

Results

Targeted Disruption of the *Gsn* Gene

A 12 kb portion of the murine *Gsn* gene was isolated from a BALB/c genomic library, encompassing the plasma gelsolin-specific exon 3 and common exons 4, 5, and 6 (Figure 1A). To disrupt translation of both cytoplasmic and plasma forms of gelsolin, the neomycin resistance (*neo*^{r}) cassette (Thomas and Capecchi, 1987; Mortensen et al., 1991) was inserted into the first common exon 60 bases downstream of the initiator methionine. The herpes simplex virus thymidine kinase (HSV–TK) cassette was then positioned on the 3′ side of the construct to provide negative selection. The gene-targeting construct was electroporated into J1 embryonic stem (ES) cells (Li et al., 1992), and 57 double-resistant clones (G418 and FIAU) were selected. Southern blot analysis showed that five of these clones displayed evidence for homologous recombination of the disrupted gelsolin construct into the native murine *Gsn* gene. Three of the clones were injected into blastocysts, and two gave germline transmission (Figures 1B and 1C). Interbreeding of heterozygotes revealed that mice homozygous for the gelsolin mutation were viable.

Analysis of *Gsn* Expression in the Targeted Mice

Gsn mRNA was undetectable by Northern blot analysis of a spectrum of tissues from homozygous *Gsn*$^-$ animals (Figure 2A, top). Minor amounts of an RNA species larger than that of normal *Gsn* mRNA hybridized to a *Gsn* probe, and this band also hybridized to a *neo*^{r} probe (Figure 2A, middle), suggesting that the transcript represented a read-through message product nonfunctional with respect to production of normal gelsolin protein. Western blot analysis failed to detect gelsolin expression in the tissue extracts of the homozygous *Gsn*$^-$ mice (Figure 2B, left). A gelsolin purification protocol (Kurokawa et al., 1990), which efficiently concentrated gelsolin from plasma of wild-type mice, yielded on SDS–polyacrylamide gels no protein with the mobility of gelsolin detectable by silver staining or Western blotting when performed on the plasma of *Gsn*$^-$ mice (Figure 2B, right). In addition, a fluorimetric assay was used to evaluate the actin filament–severing activity in the serum from these mice (Kwiatkowski et al., 1989). Heterozygous mice showed severing activity similar to that seen in wild-type mice and humans (Janmey and Lind, 1987). *Gsn*$^-$ mouse serum had no detectable severing activity (Figure 2C).

Viability, Fertility, and General Pathology

Breeding of the (+/−) animals yielded (−/−) offspring at the expected Mendelian segregation ratio (see Figure 1C). The oldest *Gsn*$^-$ homozygotes have now reached the age of 12 months and show no apparent morbidity in comparison with wild-type littermates. Histological analyses of bone marrow, brain, liver, lungs, heart, kidneys, intestine, testes, and spleen from *Gsn*$^-$ animals at the age of 3 months have shown no gross or microscopic anatomic abnormalities. Analysis of peripheral blood counts, however, showed a significant increase ($p < 0.01$) in total leukocyte count (5700 ± 1500 versus 3400 ± 1200 [SD] cells/μl) and a tendency toward a higher neutrophil fraction (17.2% ± 10.0% versus 10.8% ± 6.2% [SD]) in the *Gsn*$^-$ mice as compared with wild type.

Platelet Function in *Gsn*$^-$ Mice Is Altered

Since previous studies have implicated gelsolin-mediated actin filament severing in the shape changes accompanying the activation of blood platelets (Hartwig, 1992), the platelet function of the *Gsn*$^-$ mice was investigated in detail. The tail bleeding times of *Gsn*$^-$ mice were on average about twice as long as those of wild-type littermates (wild-type, 162 ± 101 s, n = 9; *Gsn*$^-$, 348 ± 214 s, n = 8; $p < 0.05$). In addition, the *Gsn*$^-$ animals displayed a tendency toward persistent, slow bleeding and rebleeding after initial cessation, as is commonly observed in human disorders of platelet function.

To assess the consequences of a lack of gelsolin on platelet function in vitro, the ability of resting mouse platelets to remodel their actin arrays when activated was determined. Actin remodeling in human blood platelets occurs in two general stages (Hartwig, 1992). Preexisting filaments are first severed in a calcium ion–dependent fashion. Then the severed filaments are uncapped to generate

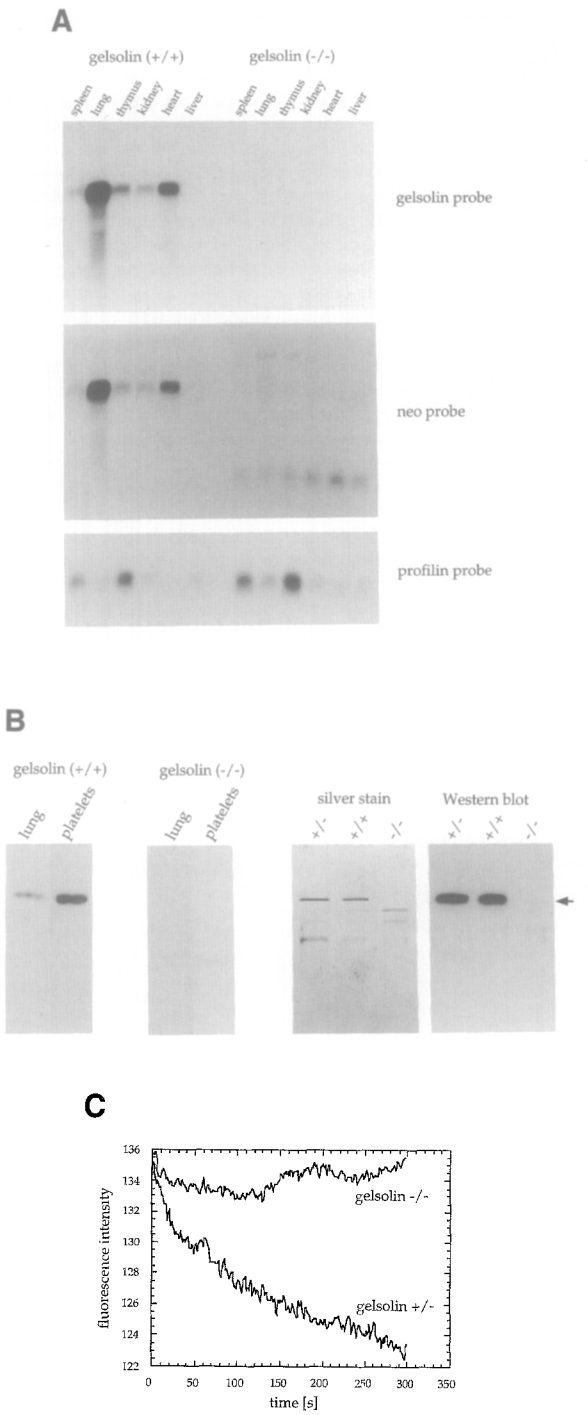

Figure 2. *Gsn*⁻ Mice Do Not Express Gelsolin

(A) Northern blot analysis of six tissues from wild-type and *Gsn* (−/−) mice, using probes for *Gsn*, *neo*ʳ, and profilin (control). Total RNA (10 μg) was loaded on a denaturing gel and transferred to GeneScreen Plus, and the same blot was probed sequentially with the three probes. The profilin probe is from the human profilin I gene (Kwiatkowski and Bruns, 1988) and serves to verify equal loading of RNA from wild-type and (−/−) mice.

(B) On the left, immunoblot analysis of two tissues from wild-type and (−/−) mice, using a polyclonal antibody prepared against murine gelsolin. On the right, silver stain and immunoblot analysis of partially purified gelsolin from heterozygote, wild-type, and homozygote *Gsn*⁻ mice. Gelsolin was partially purified from 90 μl of murine serum by using DEAE–Sepharose (Kurokawa et al., 1990). Half of the preparation was silver-stained, the remainder transferred for immunoblot analysis.

(C) F-actin severing assay of serum from heterozygote and *Gsn* (−/−) mice. Fluorescence intensity in arbitrary units is plotted over time after addition of serum to pyrene–F-actin. The (−/−) curve is the average of four observations; the (+/−) curve is the average of two observations.

nucleation sites for rapid actin assembly. This process leads to a net increase in the total actin filament content from 40% of total platelet actin in the resting state to 70%–80% of all actin, following activation. The larger number of filaments in activated platelets can be detected by an enhanced ability of permeabilized cells to accelerate assembly of monomeric actin (nucleation). *Gsn*⁻ platelets had resting actin filament contents 13% higher than heterozygous littermates (Figure 3E), although the nucleation activities of lysed resting *Gsn*⁻ and wild-type platelets were not distinguishable (Figure 3F). Following activation, F-actin concentrations rose to similar levels in wild-type and *Gsn*⁻ platelets. However, the number of actin nuclei generated in activated *Gsn*⁻ platelets was much smaller than that seen in wild-type platelets (Figure 3F). These findings are consistent with diminished capping and severing activities in *Gsn*⁻ platelets. We obtained further evidence for a severing defect in *Gsn*⁻ platelets by comparing their morphology with that of wild-type platelets during glass activation in the presence of cytochalasin B (cytoB) (Figures 3A–3D). CytoB binds to the barbed ends of actin filaments, strongly inhibiting filament elongation by subunit addition, but does not affect severing by gelsolin. Thus, cytoB permits dissection of the actin filament–severing phase of platelet activation from subsequent actin filament assembly. CytoB-treated resting platelets from wild-type mice respond to centrifugation onto glass by spreading into flat pancake forms (Figure 3A). The spreading results from a glass-induced activation that leads to actin filament severing (Hartwig, 1992), allowing centrifugal force to flatten the cell. As shown in Figure 3C, the cortex of flattened wild-type platelets contains numerous short filaments with free ends. In contrast, cytoB-treated platelets from *Gsn*⁻ mice remain compact and flatten poorly in response to centrifugation onto glass (Figure 3B), because their internal filament structure remains continuous (Figure 3D). The surface area of activated wild-type platelets was $9.85 \times 10^{-12} \pm 1.95 \times 10^{-12}$ m² versus $3.49 \times 10^{-12} \pm 1.01 \times 10^{-12}$ m² for *Gsn*⁻ platelets ($n = 100$; $p < 0.001$).

Inflammatory Response and Leukocyte Function

Gelsolin comprises nearly 1% of total cell protein in neutrophils (Yin and Stossel, 1979), suggesting that these immune effector cells might have abnormal function in the *Gsn*⁻ mice. To assess neutrophil recruitment to inflammatory sites, we treated mice with intraperitoneal thioglycollate and sampled the inflammatory exudate. At 2 hr and 3 hr after intraperitoneal injection, differences in the total amount of leukocytes (>95% neutrophils) in the peritoneum were seen (Figure 4A). To confirm these observa-

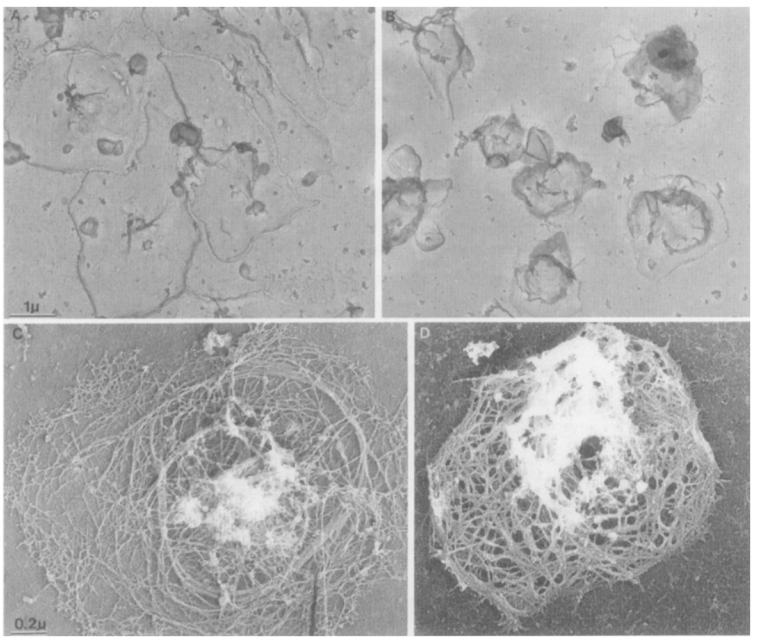

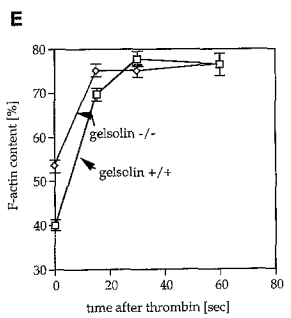

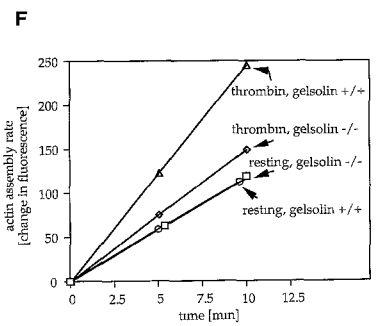

Figure 3. Abnormal Platelet Structure in the *Gsn*⁻ Mice

(A–D) Wild-type mouse platelets, centrifuged onto glass coverslips in the presence of cytoB (A), flatten because contact with glass induces a calcium ion–dependent fragmentation of cortical actin (Hartwig, 1992). *Gsn*⁻ platelets, however, compress poorly under these conditions (B), although their shapes distort from the resting discoid form. Cytoskeletons prepared in the presence of cytoB from wild-type mouse platelets contain many short actin filaments (C), while cytoskeletons from *Gsn*⁻ platelets are composed of long actin filaments (D).

(E) F-actin content of resting and thrombin-activated (1 U/ml) wild-type (+/+) and *Gsn*⁻ (−/−) platelets. Each data point represents four observations on independently prepared platelets subjected to FACS. The difference between values at time 0 is statistically significant ($p < 0.01$).

(F) Actin filament nucleation activity in lysates from resting or thrombin-activated wild-type and *Gsn*⁻ platelets, as measured by the increase in fluorescence due to assembly of pyrene–actin into filaments. The increase in actin assembly rate of thrombin-stimulated *Gsn*⁻ platelets was only 25% of that of wild-type platelets. Because of the limited number of platelets available, each curve represents the entire collected platelets pooled from three mice divided into three aliquots for the three time points. The data shown are from a single representative experiment.

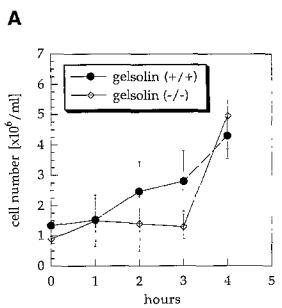

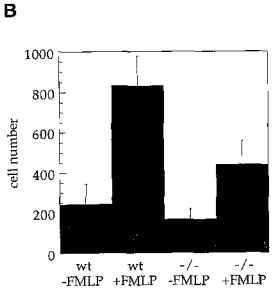

tions, a second cohort of animals was examined at the 3 hr time point, and significant differences were again seen ([+/+], $5.00 \times 10^6 \pm 1.73 \times 10^6$ cells/ml; [−/−], $2.42 \times 10^6 \pm 0.47 \times 10^6$ cells/ml, mean ± SD, $p = 0.02$). These differences disappeared at later time points, suggesting that gelsolin was important in the early phases of neutrophil recruitment. This difference was also remarkable in that the number of neutrophils circulating in the peripheral blood was approximately twice as high in the *Gsn*⁻ mice as in the wild type. Neutrophils isolated from the peritoneal exudates migrated significantly less rapidly ($p < 0.01$) in

Figure 4. Leukocyte Migration Is Impaired in the *Gsn*⁻ Mice

(A) The number of cells/ml observed in peritoneal exudates from wild-type (+/+) and *Gsn*⁻ (−/−) mice is plotted over time, following intraperitoneal administration of thioglycollate. Mean and SD for leukocyte values from three animals are shown.

(B) Migration of peritoneal neutrophils across a Boyden chamber is shown for wild-type (+/+) and *Gsn*⁻ (−/−) mice. Means ± SD for five experiments are shown.

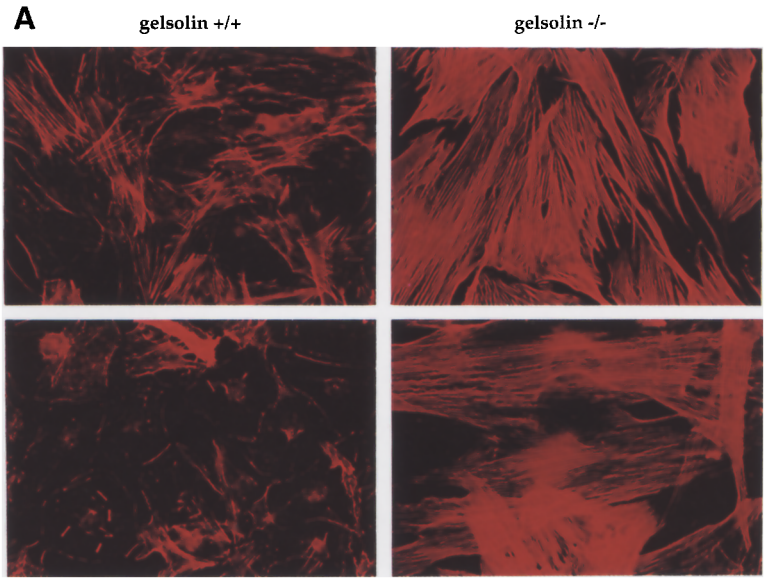

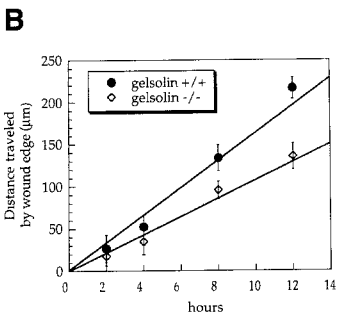

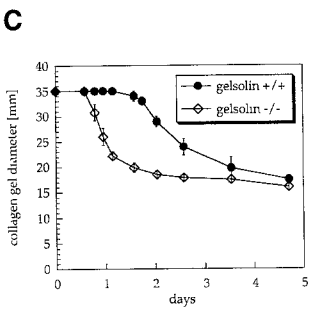

Figure 5. Abnormal *Gsn*⁻ Dermal Fibroblast Structure, Motility, and Contractility

(A) Compared with wild-type (left), *Gsn*⁻ (right) fibroblasts have much more prominent actin stress fiber patterns (top) that are poorly responsive to serum deprivation (bottom). The actin stress fibers are visualized with rhodamine–phalloidin. Serum deprivation was performed by incubation in DMEM media alone for 16 (wild-type) or 32 (*Gsn*⁻) hr.

(B) *Gsn*⁻ (−/−) fibroblasts migrate more slowly than wild type (+/+) into a wound made in a subconfluent tissue culture dish. The results are significantly different at 8 and 12 hr ($p < 0.01$). Standard error bars are shown.

(C) Wild-type (+/+) and *Gsn*⁻ (−/−) fibroblasts have differing contractile ability in collagen gels. The results are significantly different from day 1 through day 3 ($p < 0.01$).

Boyden chamber assays of chemotaxis than wild-type neutrophils did (Figure 4B), also consistent with a migration defect due to the lack of gelsolin.

Fibroblast Function

Dermal fibroblasts cultured from 8-week-old *Gsn*⁻ mice were 5.5 times larger in surface area than wild-type cells (*Gsn*⁻, $2756 \times 10^{-12} \pm 1263 \times 10^{-12}$ m²; wild-type, $517 \times 10^{-12} \pm 281 \times 10^{-12}$ m²; $n = 25$, $p < 0.001$) and contained 1.45 times the total protein content of control cells. Moreover, they had markedly accentuated actin stress fiber arrays in comparison with wild-type cells (Figure 5A, top). Stress fiber formation in fibroblasts is dependent on the presence of lysophosphatidic acid in serum under usual culture conditions, activating the GTP-binding protein rho (Ridley and Hall, 1992). Deprivation of serum led to a marked reduction in stress fibers in fibroblasts from wild-type mice (Figure 5A, bottom left) but had little effect on stress fibers in *Gsn*⁻ fibroblasts (Figure 5A, bottom right). The stress fibers of *Gsn*⁻ fibroblasts were also more resistant to cytoB treatment (data not shown) than the stress fibers of wild-type cells. The *Gsn*⁻ fibroblasts also filled in a defect in a confluent tissue culture dish more slowly (Figure 5B), and migrated through filters in a Boyden chamber assay significantly more slowly ([+/+], 138 ± 59 cells/well; [−/−], 20.3 ± 6.7 cells/well; mean ± SD, $n = 14$; $p < 0.01$) than wild-type fibroblasts. However, the *Gsn*⁻ fibroblasts were more active than wild-type fibroblasts in contracting a collagen gel (Figure 5C), possibly owing to the increased extent and number of actin stress fibers.

In contrast with the findings in fibroblasts of adult mice, fibroblasts derived from 15-day-old wild-type and *Gsn*⁻ embryos had no observable differences in size, volume, actin filament organization, or response to growth factor deprivation or cytoB treatment (data not shown). In addition, the *Gsn*⁻ embryonic fibroblasts displayed reduced collagen gel contraction compared with that of wild-type fibroblasts, in contrast with the observations made on the dermal fibroblasts from adult mice.

Expression of Gelsolin during Embryonic Development

To investigate the embryonic viability of *Gsn*⁻ mice, we examined the expression of gelsolin in wild-type mice during embryogenesis by using Western and Northern blots. In wild-type feeder layer–independent ES cells grown in the presence of leukemia inhibitory factor (LIF), no gelsolin expression was detectable by use of a polyclonal anti-

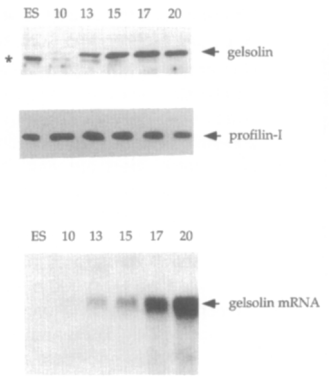

Figure 6. Expression of Gelsolin during Embryonic Development

Protein lysates were prepared from ES cells and different stage embryos (age in days is shown). Equal amounts of protein were subjected to SDS–PAGE, transferred, and probed with a polyclonal anti-gelsolin antibody (top) or a polyclonal anti-profilin I antibody (middle). Equal amounts of total RNA (15 μg) from ES cells and different stage embryos were run on a denaturing gel, transferred to gene screen plus, and hybridized with a *Gsn* cDNA probe (bottom).

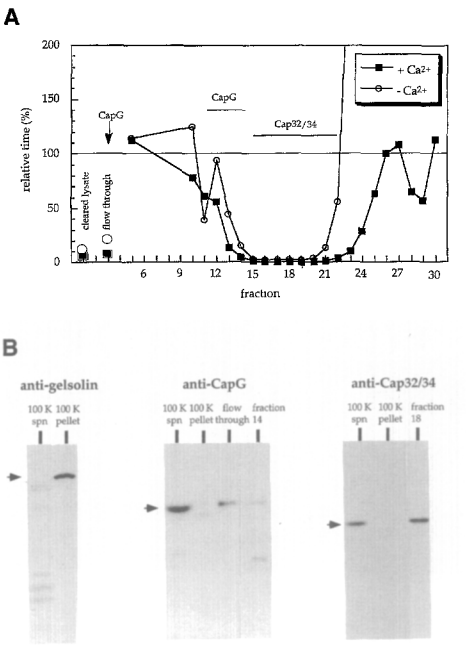

Figure 7. Viscosity-Decreasing Activities in *Gsn*⁻ ES Cell Extracts

(A) A cleared lysate from *Gsn*⁻ ES cells was fractionated on a DE-52 anion exchange resin using a linear 0–500 mM NaCl gradient. Fractions were tested in the presence of 0.2 mM $CaCl_2$ (plus Ca^{2+}) or 1 mM EGTA (minus Ca^{2+}) for their effects in a low shear viscosity assay. A shorter relative time correlates with reduced viscosity of the actin gel. Reduction in viscosity is evident in the flowthrough material and in fractions 15–21. The relative positions of elution of CapG and Cap32/34 on the basis of immunoblot analysis are shown.

(B) Western blot of fractions from the DE-52 column. Aliquots were separated by 10% or 15% SDS–PAGE, transferred to Immobilon P, and probed with a polyclonal anti-gelsolin antibody, a polyclonal anti-CapG antibody, or a polyclonal anti-Cap32/34 protein antibody. Representative immunoreactive bands are shown and indicated by arrows. The 80 kDa protein cross-reacting with the anti-gelsolin antibody was found exclusively in the 100,000 × g pellet and not in the supernatant (spn). CapG is present in the flowthrough and fraction 14. Cap32/34 is seen in the lysate and fraction 18.

gelsolin antibody. In embryo lysates, gelsolin expression was very low at day 10, increased by day 13, and continued to rise thereafter (Figure 6). However, we also observed that an immunologically cross-reactive band of apparent molecular weight 80 kDa (Figure 6, asterisk) was seen in ES cell extracts through use of the polyclonal anti-gelsolin antisera. The intensity of this band decreased during development but was still detectable at days 10 and 13. This protein was not derived from the *Gsn* gene, since the same band was visible in extracts from ES cells homozygous for the disrupted *Gsn* gene (data not shown). Profilin I (Kwiatkowski and Bruns, 1988), another actin-binding protein, was expressed at all stages of embryonic development. Northern blot analysis confirmed the lack of *Gsn* expression in ES cells. In whole embryo RNA preparations, *Gsn* mRNA levels were very low at day 10 and steadily increased from day 13 through birth (Figure 6).

No Severing Activity Is Detectable in *Gsn*⁻ ES Cell Extracts

To examine the possibility that a gelsolin-related severing protein is expressed in early embryogenesis, we analyzed the expression of proteins modulating actin filament dynamics in *Gsn*⁻ ES cells. ES cell extracts were prepared by hypotonic lysis with freeze-thawing. Following high speed centrifugation to pellet insoluble cytoskeleton and nuclei, the lysate was fractionated by anion exchange chromatography, and fractions were examined for effects on actin filament gels. As seen in Figure 7A, both the unfractionated cleared lysate and several column fractions reduced the viscosity of actin gels in a low shear viscosity assay (MacLean-Fletcher and Pollard, 1980) in a Ca^{2+}-independent manner. However, both a dilutional pyrene F-actin severing assay and an actin nucleation assay (Kwiatkowski et al., 1989) failed to detect any gelsolin-like activity in any of the fractions (data not shown). The absence of severing activity in the pyrene–F-actin assay, and the presence of strong actin viscosity–reducing activity in the low shear viscosity assay in the flowthrough and fractions 15–21, suggested that two distinct capping proteins were present in these ES cell extracts. Immunoblot analysis was used to demonstrate (Figures 7A and 7B) that the capping proteins CapG and Cap32/34 were present in several fractions. CapG was seen predominantly in the flowthrough, while Cap32/34 was seen in fractions 15–21. To confirm that Cap32/34 was the only capping protein present in the broad peak of viscosity-reducing activity in fractions 17–21, these fractions were pooled and subjected to two further column fractionations on Hydroxyapatite and Sephacryl S-300. Both purification steps yielded a single peak of viscosity-reducing activity, and immunoblot analysis confirmed that these correlated with the presence of Cap32/34. Therefore, Cap32/34 was quite likely the sole factor accounting for the reduced viscosity of the actin gels made with fractions 15–21. The capping activity in the flowthrough can be attributed to CapG, although other

proteins with similar functional activity might also be present. The M_r 80 kDa protein cross-reactive with polyclonal anti-gelsolin antibodies was found to fractionate exclusively in the insoluble pellet. The potential activity of this protein on actin gels and in severing actin filaments could therefore not be examined. The increase in actin viscosity in the late fractions from the anion exchange column is most likely due to the presence of nonmuscle α-actinin, which is known to elute at higher salt concentration and to cross-link actin filaments in the absence of Ca^{2+} but not in the presence of μM concentrations of Ca^{2+}.

To confirm that a gelsolin homolog would be detected by the methods used, we analyzed extracts from wild-type embryo fibroblast cells. The dilutional pyrene–F-actin severing assay easily detected the presence of gelsolin in these extracts (data not shown). We estimate that the presence of 5% of the severing activity seen in wild-type cell extracts could be detected by this assay.

Discussion

We have generated *Gsn*$^-$ mice that have no apparent defect in oogenesis, spermatogenesis, early embryogenesis, or general reproductive fitness. However, the adult animals display defects in hemostasis and platelet activation, inflammatory response and leukocyte motility, and dermal fibroblast function in vitro.

Initially, the viability and normal fertility of *Gsn*$^-$ mice was surprising, given the high level of gelsolin expression in many adult murine tissues (Kwiatkowski et al., 1988a). However, the existence of several members of the gelsolin family and many other proteins with partial functional similarity has suggested from the outset that these other proteins could provide functional compensation for a complete lack of gelsolin expression. We have demonstrated that gelsolin expression is low until day 15 of embryonic murine development (Figure 6), and moreover, that neither gelsolin nor any other soluble actin filament–severing protein is expressed in ES cells at a detectable level (Figure 7). In Xenopus, a moderately abundant protein with actin filament–severing, –capping, and –nucleating activity was purified and cloned from oocytes that had 70% amino acid identity to human gelsolin (Ankenbauer et al., 1988). These observations suggested that gelsolin plays an important role in the Ca^{2+}-dependent gelation and contractility processes that occur during amphibian oogenesis and embryogenesis. On the other hand, our results demonstrate that at least in mouse and probably therefore in all mammals, gelsolin does not play an essential role in oogenesis or embryogenesis.

Among the diverse proteins that bind actin (Hartwig and Kwiatkowski, 1991), two families of proteins seem particularly likely to account for the normal motility of cells in embryogenesis in *Gsn*$^-$ mice: the capping protein family and the family of small actin monomer–binding proteins with weak filament-severing activity. There are two widely expressed proteins with filament-capping activity that do not sever actin filaments (Weeds and Maciver, 1993): Cap32/34 (also known as capping protein, β-actinin, and CapZ) (Maruyama, 1965; Isenberg et al., 1980; Casella et al., 1987; Hartmann et al., 1989) and CapG (Southwick and DiNubile, 1986; Yu et al., 1990). Removal of a capping protein from actin filament barbed ends, a reaction promoted by membrane PPI for these proteins as well as filament-severing proteins (Hartwig and Kwiatkowski, 1991; Weeds and Maciver, 1993), leads to net actin assembly by subunit addition onto the freed barbed ends. As we have demonstrated that both Cap32/34 and CapG are expressed at appreciable levels in functional assays of ES cell extracts, we conclude that capping and uncapping of actin filaments may be the preferred mechanism by which embryonic cells reorganize their actin cytoskeleton. This mechanism would allow the slow movements that occur during early embryonic development.

The family of small actin monomer–binding proteins with weak filament-severing activity includes two widely and highly expressed members, actin depolymerizing factor (ADF)/destrin (Bamburg et al., 1980) and cofilin (Yonezawa et al., 1985), that have 70% identical sequences (Abe et al., 1990). Both proteins bind to the sides of actin filaments in a stoichiometric manner at pH 7.0 or less, but prefer to bind to actin monomers at pH 7.5 or above (Yonezawa et al., 1985; Hawkins et al., 1993). At higher pH (>7.5, maximal at 8.0), both proteins can sever actin filaments in a substoichiometric manner. However, the rate of severing is slow and has efficiency less than 0.1% of that of gelsolin. In addition, cellular pH is rarely over 7.4 in mammalian cells, suggesting that these proteins are unlikely to contribute to actin filament dynamics through their severing activity. We detected cofilin mRNA in ES cells (data not shown), but the described functional properties explain why its severing activity was not detected in our assays of ES cell extracts. ADF/destrin and cofilin seem less likely to be important components of motility in embryogenesis, although the gene encoding cofilin is essential in yeast (Moon et al., 1993).

Despite their apparently normal development and reproductive function, the *Gsn*$^-$ mice have impaired physiological responses in at least two systems that require rapid motile events. One of these is a prolonged bleeding time most likely due to diminished severing of actin filaments in *Gsn*$^-$ platelets and a corresponding reduction in the platelet shape change response. The residual capacity of *Gsn*$^-$ platelets to undergo a shape change may be due to the presence of adseverin, a gelsolin family member, at about 20% of the level of gelsolin (Rodríguez Del Castillo et al., 1992), or the presence of Cap32/34 (K. Barkalow and J. H. H., unpublished data), or both. The doubling of the bleeding time is roughly comparable to the effects of aspirin administration in humans, which is well tolerated, and may explain why hemorrhagic complications were not seen in the *Gsn*$^-$ mice.

Gsn$^-$ mice responded more slowly than wild-type mice to a strong inflammatory stimulus, intraperitoneal thioglycollate instillation. The kinetics of leukocyte accumulation in *Gsn*$^-$ mice were similar to those observed in P-selectin knockout mice (Mayadas et al., 1993). The slow emigration of leukocytes could be related to a reduced cell migration rate, since the exudate *Gsn*$^-$ leukocytes showed slower locomotion than wild-type cells in vitro. The sharp increase

in peritoneal leukocytes seen at 4 hr (Figure 4A) could simply reflect the delayed arrival of a complement of leukocytes appropriate to the inflammatory stimulus. The high levels of circulating leukocytes in general and of neutrophils in particular suggest that basal leukocyte trafficking in *Gsn*$^-$ animals is abnormal. Diminished influx of cells into tissues could result in higher circulating cell counts. Nevertheless, under pathogen-free housing conditions, the *Gsn*$^-$ mice do not appear to be unusually susceptible to infection.

Cultured *Gsn*$^-$ fibroblasts had striking morphological abnormalities consistent with impaired actin depolymerization, most simply explained by a reduction in cytoplasmic actin filament–severing activity. Their actin stress fibers were abnormally large and resistant to mobilization by stimuli that dissolve such fibers in wild-type cells. On the other hand, the *Gsn*$^-$ fibroblasts were hypercontractile, presumably because the large stress fibers are sarcomeric in function. Rho, a ras family member, has recently been shown to be the central signaling molecule by which stress fibers are induced in Swiss 3T3 cells in response to stimulation with lysophosphatidic acid (Paterson et al., 1990; Ridley and Hall, 1992). Activation of rac, another ras family member, leads to ruffling activity in Swiss 3T3 cells (Ridley et al., 1992). Apart from rho activation, to our knowledge lack of gelsolin expression is the only alteration known to result in stress fiber enhancement in fibroblasts. Since rho and rac have contrasting effects on actin filament organization, the comparable cellular features of *Gsn*$^-$ fibroblasts and wild-type fibroblasts following rho activation/microinjection suggest that gelsolin and rac are in a common signaling pathway from receptor to the actin cytoskeleton. Whether gelsolin is directly or indirectly affected by rac or other family members is currently under investigation. Stress fibers are not generally observed in fibroblasts in vivo, but do appear during wound healing (Welch et al., 1990). Therefore, the function of *Gsn*$^-$ fibroblasts in vivo may be adequate under normal conditions but could have significant deficiencies during the healing process. Fibroblasts isolated from wild-type day 15 embryos and *Gsn*$^-$ embryos do not display the differences observed for adult dermal fibroblasts. The simplest explanation for this finding is that although both cultured cells are phenotypically fibroblasts, they differ in actin filament organization, mechanisms of motility, and protein expression.

We have shown that *Gsn*$^-$ mice are also deficient in the plasma isoform of gelsolin, and that serum from these mice shows no detectable actin filament–severing activity. Plasma gelsolin has been proposed to function as an actin scavenger after acute tissue damage and actin release (Lind et al., 1986; Lee and Galbraith, 1992). The *Gsn*$^-$ mice we have generated will allow this hypothesis to be tested and will clarify whether F-actin severing is important or whether the actin monomer–binding protein (vitamin D–binding protein) (Young et al., 1987), which is also present in serum at high concentrations, is sufficient to protect the animal from circulating actin during injury.

In summary, gelsolin is not essential for mammalian development but is important for maximal motile responses associated with aspects of host defense. In slow-moving cells and in early embryonic development, capping and uncapping of actin filaments rather than severing appears to be the preferred mechanism of remodeling the actin cytoskeleton. The existence of viable *Gsn*$^-$ animals with blunted hemostatic and inflammatory responses also suggests that gelsolin might represent a target for antithrombotic and anti-inflammatory therapy.

Experimental Procedures

Generation of *Gsn*$^-$ Mice and ES Cells

A murine *Gsn* genomic fragment was isolated from a BALB/c library (L. Clayton), and an 8 kb HindIII fragment containing exons 4–6 and the 5′ upstream region was subcloned in pGemblue. The vector was opened at the unique BglII site in the first common exon 4 for plasma and cytoplasmic gelsolin, and the *neo* cassette was inserted as a BglII–BamHI fragment. The disrupted genomic HindIII fragment was ligated into the HSV–TK vector such that the short arm of the targeting sequence was located next to the HSV–TK cassette. The targeting vector was linearized with SalI, and 20 μg was transfected by electroporation into 10^7 J1 ES cells (Li et al., 1992), which were maintained on a feeder layer of *neo*^{r} embryonic fibroblasts in the presence of 500 U/ml LIF. Fifty-seven clones were selected with G418 (200 μg/ml) and FIAU (2 μM) and were evaluated by Southern blot analysis of DNA after minimal passage. Five clones displayed a novel 5.8 kb BamHI allele predicted to occur after homologous recombination. Analysis with a variety of enzymes provided no evidence for other untoward genetic events in these five ES cell sublines. Three sublines were injected into d3.5 C57BL/6 or BALB/c blastocysts and the blastocysts transferred into pseudopregnant females. Chimeric mice were bred with C57BL/6 or BALB/c mice and agouti offspring analyzed for the disrupted *Gsn* allele. Tail snips were used to prepare DNA by standard methods for Southern blot analysis (Laird et al., 1991).

The *Gsn* gene was similarly disrupted in the feeder layer–independent ES cell line CCE (Schwartzberg et al., 1989). To generate ES cells homozygous for the *Gsn* mutation, cells heterozygous for the *Gsn* mutation (10^5 cells) were treated with high concentrations of G418 (2 mg/ml) (Mortensen et al., 1991). Ten clones were isolated after selection, of which nine showed the disappearance of the normal *Gsn* allele by Southern blot analysis. The absence of gelsolin expression was confirmed by immunoblot analysis of protein extracts from wild-type and *Gsn*$^-$ ES cells differentiated for 7 days in the absence of LIF.

Platelet Analysis

Unactivated platelets were obtained from mice by laparatomy and aspiration from the inferior vena cava into a solution of 0.15 M sodium citrate, 0.043 M citric acid, 20 mg/ml glucose (pH 4.6). Platelets were gel purified (Hartwig, 1992) and incubated in 10 μM cytoB (Sigma) for 10 min prior to centrifugation onto glass coverslips for the electron microscopic studies (Hartwig, 1992). Platelet cytoskeletons were prepared by extraction in 1% Triton X-100. Cells and cytoskeletons were prepared for the electron microscope by rapid freezing, freeze drying, and metal coating (Hartwig, 1992).

For actin filament content measurements, platelets were fixed in 2% formaldehyde and permeabilized with 0.1% Triton X-100 in 10 μM tetramethylrhodamine B isothiocyanate (TRITC)–phalloidin (Sigma). Bound phalloidin was quantitated by fluorescence-activated cell sorting (FACS) (Howard and Oresajo, 1985). For the actin filament nucleation assay, 1.65×10^7 platelets were extracted in 0.075% Triton X-100 in PHEM buffer (Hartwig, 1992) and mixed with 1 μM pyrene–actin in 10 mM Tris–HCl (pH 7.5), 0.1 M KCl, and 2 mM $MgCl_2$. The fluorescence was monitored with a Perkin-Elmer fluorimeter.

Inflammatory Response and Neutrophil Studies

Sodium thioglycollate (1 ml at 2.4%) was injected into the peritoneal cavity of 6- to 8-week-old mice. Mice were sacrificed at serial timepoints and the peritoneal cavity rinsed with 5 ml of phosphate-buffered saline (PBS) to permit complete collection and quantitation of the resulting inflammatory exudate. Neutrophils collected at hour 5 of this process were then washed three times in PBS with 5% bovine serum albumin (BSA) and placed in the top of a two-compartment Boyden chamber

apparatus with 1 μM formyl-methionyl-leucyl-phenylalanine (FMLP) as chemoattractant in the lower wells and a 5 μm (pore size) PVDV filter. After a 90 min incubation at 37°C, cells were counted on the lower surface of the filter after fixation in methanol and staining with Giemsa.

Fibroblast Culture and Experiments

Dermal fibroblasts were cultured as explants from the cutaneous tissues of 6-week-old adult mice and were maintained in Dulbecco's modified Eagle's medium (DMEM) with 10% fetal calf serum (FCS). Embryonic fibroblasts were cultured from day 15 embryos as described (Abbondanzo et al., 1993) in similar media. To visualize the actin filament architecture, cells were cultured on glass coverslips coated with poly L-lysine, fixed with acetone at −20°C for 5 min, incubated in 1 μg/ml TRITC–phalloidin (Sigma), rinsed, and viewed on an Olympus BH2 microscope. Surface area measurements of stained cells were made by image analysis using the public domain software Image, version 1.51. Tissue culture motility measurements were made by wounding a subconfluent culture dish with a sterile 18 gauge needle. The margins were measured over time by using an eyepiece micrometer (Cunningham et al., 1991). Collagen was prepared from rat tail (Grinnell and Lamke, 1984), and 2×10^5 cells were then plated in a polymerizing collagen gel (1 mg/ml) in the presence of 20% FCS. Contraction of the collagen gel was observed and quantitated visually over a period of 7 days.

Tail Bleeding Times

A 1 cm piece was snipped from the tail of a mouse and the tail immediately placed in a clear tube with 10 ml of 37°C prewarmed saline. Blood flow was observed, and the endpoint of bleeding was defined as the permanent interruption of blood flow for more than 15 s.

Lysates from Different Stage Embryos

Wild-type mice were mated, and pregnant females were sacrificed after 10, 13, 15, and 17 days postcoitum. Embryos were dissected, washed in PBS, and snap-frozen in liquid nitrogen. Newborns (day 20) were killed by cervical dislocation and stored in liquid nitrogen. For preparation of protein extracts, frozen embryos were placed in 1 ml of ice-cold extraction buffer (0.5% Triton X-100, 50 mM Tris–HCl [pH 7.4], 150 mM NaCl, 2 mM EGTA, 5 mM EDTA, 1 mM benzamidine, 0.5 mM phenylmethylsulfonyl fluoride [PMSF]) and homogenized by 20–30 strokes with a tight-fitting conical-shaped douncer. The lysate was spun for 30 min at 100,000 × g, the supernatant concentration was determined by Bradford assay, and equal amounts of protein were separated by SDS–polyacrylamide gel electrophoresis (PAGE).

Fractionation of ES Cell Extracts and Actin Gel Viscosity Assay

Packed *Gsn*$^-$ ES cells (2 ml) were resuspended in swelling buffer (5 mM EDTA, 2 mM EGTA, 2 mM benzamidine, 1 mM dithiothreitol [DTT], 5 mM Tris–HCl [pH 8.0]), left for 10 min on ice, and lysed by freeze–thawing and three 10 s pulses with a sonicator probe. The lysate was cleared by a 100,000 × g spin and the supernatant loaded on DE-52 (Whatman) resin and preequilibrated in TEDABAP (10 mM Tris–HCl [pH 8.0], 2 mM EGTA, 0.1 mM DTT, 0.01% sodium azide, 1 mM benzamidine, 0.1 mM ATP, 0.5 mM PMSF). The resin was washed with 10 column vol of TEDABAP, and proteins were eluted with a 0–500 mM NaCl gradient in TEDABAP. Aliquots of all fractions were tested in the falling ball assay (MacLean-Fletcher and Pollard, 1980) to detect viscosity-decreasing activity. Of each fraction, 20 μl (10–20 μg of protein) was copolymerized for 1 hr with monomeric rabbit skeletal muscle actin (final concentration, 9 μM) in a 100 μl capillary pipette in the presence of 10 mM imidazole (pH 7.6), 2 mM $MgCl_2$, and 0.2 mM $CaCl_2$ or 1 mM EGTA. Viscosity is determined by measuring the time for a steel ball to fall in the capillary. Falling times are normalized to the time of an actin gel alone (100%) without added protein. Severing and capping proteins decrease the falling time by reducing the viscosity of the resulting actin gel. Aliquots of all fractions were analyzed by immunoblotting using polyclonal antibodies against gelsolin, CapG, and Cap32/34.

Other Methods

RNA preparation, agarose electrophoresis, transfer, and probing were all done by standard methods.

For immunoblot analysis, proteins were separated by SDS–PAGE, transferred to Immobilon P, and probed with a rabbit polyclonal antiserum made against bacterially expressed murine gelsolin, bacterially expressed human profilin I, human CapG (provided by F. Southwick), or Cap32/34 (Schafer et al., 1992). Detection of binding was achieved with a horseradish peroxidase-conjugated secondary antibody and incubation with the enhanced chemiluminescence reagent (New England Nuclear).

For the F-actin severing assays, a 1/25 dilution of serum or 20 μl of ES cell extract (50 μg) or fractions (10–20 μg) were added to 200 nM pyrene–F-actin in 0.1 M KCl, 2 mM $MgCl_2$, 1 mM $CaCl_2$, 0.5 mM ATP, 10 mM Tris–HCl (pH 7.2), and the fluorescence was monitored with a Perkin-Elmer fluorimeter (Kwiatkowski et al., 1989). For the F-actin nucleating assay, 20 μl of ES cell extract was added to 1 μM pyrene–G-actin in similar buffer and the increase in fluorescence monitored.

Total leukocyte counts were determined after hemolysis of erythrocytes for 10 min on ice in 155 mM NH_4Cl, 10 mM NH_4CO_3, 0.1 mM EDTA (pH 7.4). Differential counts were determined by examination of Wright–Giemsa-stained blood smears. Histology was done on 5 μm sections from formaldehyde-fixed and paraffin-embedded organs stained with hematoxilin–eosin.

Acknowledgments

Correspondence should be addressed to W. W. or D. K. We thank L. Clayton, B. Tuan, R. Mortensen, P. Marks, P. Allen, J. Cooper, F. S. Southwick, and P. Janmey for assistance. This work was supported by the National Institutes of Health (HL 48743, HL 19429), Deutsche Forschungsgemeinschaft, Adolf Butenandt, the Lucille P. Markey Charitable Trust, the American Cancer Society, and the American Heart Association.

Received November 9, 1994; revised January 30, 1995.

References

Abbondanzo, S., Gadi, I., and Stewart, C. (1993). Derivation of embryonic stem cell lines. In Guide to Techniques in Mouse Development, P. Wassarman and M. DePamphilis, eds. (San Diego: Academic Press), pp. 803–822.

Abe, H., Endo, T., Yamamoto, K., and Obinata, T. (1990). Sequence of cDNAs encoding actin depolymerizing factor and cofilin of embryonic chicken skeletal muscle: two functionally distinct actin-regulatory proteins exhibit high structural homology. Biochemistry *29*, 7420–7425.

André, E., Brink, M., Gerisch, G., Isenberg, G., Noegel, A., Schleicher, M., Segall, J. E., and Wallraff, E. (1989). A *Dictyostelium* mutant deficient in severin, an F-actin fragmenting protein, shows normal motility and chemotaxis. J. Cell Biol. *108*, 985–995.

Ankenbauer, T., Kleinschmidt, J. A., Vandekerckhove, J., and Franke, W. W. (1988). Proteins regulating actin assembly in oogenesis and early embryogenesis of *Xenopus laevis*: gelsolin is the major cytoplasmic actin-binding protein. J. Cell Biol. *107*, 1489–1497.

Bamburg, J. R., Harris, H. E., and Weeds, A. G. (1980). Partial purification and characterization of an actin depolymerizing factor from brain. FEBS Lett. *121*, 178–181.

Bretscher, A., and Weber, K. (1980). Villin is a major protein of microvillus cytoskeleton which binds both G and F actin in a calcium-dependent manner. Cell *20*, 839–847.

Campbell, H. D., Schimansky, T., Claudianos, C., Ozsarac, N., Kasprzak, A. B., Cotsell, J. N., Young, I. G., de Couet, H. G., and Miklos, G. L. G. (1993). The *Drosophila melanogaster flightless-I* gene involved in gastrulation and muscle degeneration encodes gelsolin-like and leucine-rich repeat domains and is conserved in *Caenorhabditis elegans* and humans. Proc. Natl. Acad. Sci. USA *90*, 11386–11390.

Casella, J., Craig, S., Maack, D., and Brown, A. (1987). CapZ (36/32), a barbed end actin-capping protein, is a component of the Z-line of skeletal muscle. J. Cell Biol. *105*, 371–379.

Chaponnier, C., Yin, H. L., and Stossel, T. P. (1987). Reversibility of gelsolin/actin interaction in macrophages. J. Exp. Med. *165*, 97–106.

Condeelis, J. (1994). Life at the leading edge: the formation of cell

protrusions. Annu. Rev. Cell Biol. *9*, 411–444.

Cunningham, C. C., Stossel, T. P., and Kwiatkowski, D. J. (1991). Enhanced motility in NIH 3T3 fibroblasts that overexpress gelsolin. Science *251*, 1233–1236.

Diffenbach, C. W., SenGupta, D. N., Krause, D., Sawzak, D., and Silverman, R. H. (1989). Cloning of murine gelsolin and its regulation during differentiation of embyronal carcinoma cells. J. Biol. Chem. *264*, 13281–13288.

Grinnell, F., and Lamke, C. R. (1984). Reorganization of hydrated collagen lattices by human skin fibroblasts. J. Cell Sci. *66*, 51–63.

Hartmann, H., Noegel, A., Eckerskorn, C., Rapp, S., and Schleicher, M. (1989). Ca^{2+}-independent F-actin capping protein Cap32/34, a capping protein from Dictyostelium discoideum, does not show sequence homology with known actin-binding proteins. J. Biol. Chem. *264*, 12639–12647.

Hartwig, J. H. (1992). Mechanisms of actin rearrangements mediating platelet activation. J. Cell Biol. *118*, 1421–1442.

Hartwig, J. H., and Kwiatkowski, D. J. (1991). Actin-binding proteins. Curr. Opin. Cell Biol. *3*, 87–97.

Hasegawa, T., Takahashi, S., Hayashi, H., and Hatano, S. (1980). Fragmin: a calcium ion sensitive regulatory factor on the formation of actin filaments. Biochemistry *19*, 2677–2683.

Hawkins, M., Pope, B., Maciver, S., and Weeds, A. (1993). Human actin depolymerizing factor mediates a pH-sensitive destruction of actin filaments. Biochemistry *32*, 9985–9993.

Howard, T. H., and Oresajo, C. O. (1985). The kinetics of chemotactic peptide-induced change in F-actin content, F-actin distribution, and the shape of neutrophils. J. Cell Biol. *101*, 1078–1085.

Howard, T., Chaponnier, C., Yin, H., and Stossel, T. (1990). Gelsolin–actin interaction and actin polymerization in human neutrophils. J. Cell Biol. *110*, 1983–1991.

Isenberg, G., Aebi, U., and Pollard, T. (1980). An actin-binding protein from *Acanthamoeba* regulates actin filament polymerization and interactions. Nature *288*, 455–459.

Janmey, P. A., and Lind, S. E. (1987). Capacity of human serum to depolymerize actin filaments. Blood *70*, 524–530.

Kurokawa, H., Fujii, W., Ohmi, K., Sakurai, T., and Nonomura, Y. (1990). Simple and rapid purification of brevin. Biochem. Biophys. Res. Commun. *168*, 451–457.

Kurth, M., and Bryan, J. (1984). Platelet activation induces the formation of a stable gelsolin–actin complex from monomeric gelsolin. J. Biol. Chem. *259*, 7473–7479.

Kwiatkowski, D. J. (1988). Predominant induction of gelsolin and actin-binding protein during myeloid differentiation. J. Biol. Chem. *263*, 13857–13862.

Kwiatkowski, D. J., and Bruns, G. A. (1988). Human profilin: molecular cloning, sequence comparison, and chromosomal analysis. J. Biol. Chem. *263*, 5910–5915.

Kwiatkowski, D. J., Mehl, R., Izumo, S., Nadal, G. B., and Yin, H. L. (1988a). Muscle is the major source of plasma gelsolin. J. Biol. Chem. *263*, 8239–8243.

Kwiatkowski, D. J., Mehl, R., and Yin, H. L. (1988b). Genomic organization and biosynthesis of secreted and cytoplasmic forms of gelsolin. J. Cell Biol. *106*, 375–384.

Kwiatkowski, D. J., Janmey, P. A., and Yin, H. L. (1989). Identification of critical functional and regulatory domains in gelsolin. J. Cell Biol. *108*, 1717–1726.

Laird, P. W., Zijderveld, A., Linders, K., Rudnicki, M. A., Jaenisch, R., and Berns, A. (1991). Simplified mammalian DNA isolation procedure. Nucl. Acids Res. *19*, 4293.

Lamb, J. A., Allen, P. G., Tuan, B. Y., and Janmey, P. A. (1993). Modulation of gelsolin function. Activation at low pH overrides Ca^{2+} requirement. J. Biol. Chem. *268*, 8999–9004.

Lee, J., Ishihara, A., Theriot, J. A., and Jacobson, K. (1993). Principles of locomotion for simple-shaped cells. Nature *362*, 167–171.

Lee, W. M., and Galbraith, R. M. (1992). The extracellular actin–scavenger system and actin toxicity. N. Engl. J. Med. *326*, 1335–1341.

Li, E., Bestor, T., and Jaenisch, R. (1992). Targeted mutation of the DNA methyltransferase gene results in embryonic lethality. Cell *69*, 915–926.

Lind, S. E., Smith, D. B., Janmey, P. A., and Stossel, T. P. (1986). Role of plasma gelsolin and the vitamin D–binding protein in clearing actin from the circulation. J. Clin. Invest. *78*, 736–742.

Lind, S. E., Janmey, P. A., Chaponnier, C., Herbert, T., and Stossel, T. P. (1987). Reversible binding of actin to gelsolin and profilin in human platelet extracts. J. Cell Biol. *105*, 833–842.

MacLean-Fletcher, S. D., and Pollard, T. D. (1980). Viscometric analysis of the gelation of *Acanthamoeba* extracts and purification of two gelation factors. J. Cell Biol. *85*, 414–428.

Maekawa, S., Toriyama, M., Hisanaga, S., Yonezawa, N., Endo, S., Hirokawa, N., and Sakai, H. (1989). Purification and characterization of a Ca^{2+}-dependent actin filament severing protein from bovine adrenal medulla. J. Biol. Chem. *264*, 7458–7465.

Maruyama, K. (1965). A new protein-factor hindering network formation of F-actin in solution. Biochim. Biophys. Acta *94*, 208–225.

Mayadas, T. N., Johnson, R. C., Rayburn, H., Hynes, R. O., and Wagner, D. D. (1993). Leukocyte rolling and extravasation are severely compromised in P selectin–deficient mice. Cell *74*, 541–554.

Moon, A., Janmey, P., Louie, K., and Drubin, D. (1993). Cofilin is an essential component of the yeast cortical cytoskeleton. J. Cell Biol. *120*, 421–435.

Mortensen, R. M., Zubiaur, M., Neer, E. J., and Seidman, J. G. (1991). Embryonic stem cells lacking a functional inhibitory G-protein subunit ($\alpha i2$) produced by gene targeting of both alleles. Proc. Natl. Acad. Sci. USA *88*, 7036–7040.

Paterson, H., Self, A., Garrett, M., Just, I., Aktories, K., and Hall, A. (1990). Microinjection of recombinant p21rho induces rapid changes in cell morphology. J. Cell Biol. *111*, 1001–1007.

Ridley, A. J., and Hall, A. (1992). The small GTP-binding protein rho regulates the assembly of focal adhesions and actin stress fibers in response to growth factors. Cell *70*, 389–399.

Ridley, A. J., Paterson, H. F., Johnston, C. L., Diekmann, D., and Hall, A. (1992). The small GTP-binding protein rac regulates growth factor-induced membrane ruffling. Cell *70*, 401–410.

Rodríguez Del Castillo, A., Vitale, A., Tchakarov, L., and Trifaró, J.-M. (1992). Human platelets contain scinderin, a Ca^{2+}-dependent actin filament severing protein. Thromb. Haemost. *67*, 248–251.

Schafer, D., Mooseker, M., and Cooper, J. (1992). Localization of capping protein in chicken epithelial cells by immunofluorescence and biochemical fractionation. J. Cell Biol. *118*, 335–346.

Schwartzberg, P., Goff, S., and Robertson, E. (1989). Germ-line transmission of a c-*abl* mutation produced by targeted gene disruption in ES cells. Science *246*, 799–803.

Southwick, F. S., and DiNubile, M. J. (1986). Rabbit alveolar macrophages contain a Ca^{2+}-sensitive, 41,000-dalton protein which reversibly blocks the "barbed" ends of actin filaments but does not sever them. J. Biol. Chem. *261*, 14191–14196.

Stossel, T. P. (1993). On the crawling of animal cells. Science *260*, 1086–1094.

Thomas, K. R., and Capecchi, M. R. (1987). Site-directed mutagenesis by gene targeting in mouse embryo–derived stem cells. Cell *51*, 503–512.

Weeds, A., and Maciver, S. (1993). F-actin capping proteins. Curr. Opin. Cell Biol. *5*, 63–69.

Welch, M. P., Odland, G. F., and Clark, R. A. (1990). Temporal relationships of F-actin bundle formation, collagen and fibronectin matrix assembly, and fibronectin receptor expression to wound contraction. J. Cell Biol. *110*, 133–145.

Yamamoto, K., Pardee, J. D., Reidler, J., Stryer, L., and Spudich, J. A. (1982). Mechanism of interaction of *Dictyostelium* severin with actin filaments. J. Cell Biol. *95*, 711–719.

Yin, H. L., and Stossel, T. P. (1979). Control of cytoplasmic actin gel–sol transformation by gelsolin, a calcium-dependent regulatory protein. Nature *281*, 583–586.

Yin, H. L., Hartwig, J. H., Maruyama, K., and Stossel, T. P. (1981). Ca^{2+} control of actin filament length. Effect of macrophage gelsolin

on actin polymerization. J. Biol. Chem. *256*, 9693–9697.

Yonezawa, N., Nishida, E., and Sakai, H. (1985). pH control of actin polymerization by cofilin. J. Biol. Chem. *260*, 14410–14412.

Young, W. O., Goldschmidt, C. P., Emerson, D. L., Lee, W. M., Jollow, D. J., and Galbraith, R. M. (1987). Correlation between extent of liver damage in fulminant hepatic necrosis and complexing of circulating group-specific component (vitamin D–binding protein). J. Lab. Clin. Med. *110*, 83–90.

Yu, F., Johnston, P. A., Suedhof, T. C., and Yin, H. L. (1990). gCap39, a calcium ion– and polyphosphoinositide-regulated actin capping protein. Science *250*, 1413–1415.